

# Thermoelastic Performance of Copper Foil and Cu/FR-4 and Cu/PI Laminates

G. Khatibi\*, M. Klein\*, E. El-Magd \*\*, H. D. Merchant\*, B. Weiss\*, R. Wiechmann\*\*, P. Zimprich\*

\* University of Vienna, Austria; \* Gould Electronics, Eastlake, OH 44095;

\*\* Gould Electronics, Eichstetten, Germany,

\*\* RWTH Aachen, University of Technology, Aachen, Germany

## Abstract

Utilizing a micro-tensile tester and non-contacting laser-speckle correlation technique for strain measurement with nanometer resolution, elastic modulus and thermal expansion coefficient of 35 $\mu$ m electrodeposited and rolled foils are determined between 23 and 300 deg C. Careful analysis of stress-strain curve in tensile mode in the elastoplastic region has yielded accurate values of yield stress, tangent modulus, strain-hardening parameter and strain rate-hardening parameter over the whole temperature range. In conjunction with these basic thermoelastic parameters and first-order analytical relationships, it is possible to predict (i) dents and wrinkles in foil and (ii) warpage, twist and curl in laminate. Several analytical predictive models are illustrated, citing material measures to control defects (i) and (ii) in foil and laminate.

## Introduction

Conventional tensile testing of copper foil utilizes the crosshead movement monitor to ascertain strain. However, this procedure overestimates strain in the elastic regime, with a slight bending of the stress/strain curve, with the result: (i) low apparent elastic modulus, (ii) gradual elastic to plastic yield transition and (iii) somewhat imprecise definition of yield level.

Elastic modulus and yield stress of cold rolled 6mm copper plate between 23 and 450°C, using contact extensometer, has been determined by Munse and Weil (Figure 8)<sup>(1)</sup>. Employing non-contacting optical strain tracking system, essential for fragile foil sample, Fox<sup>(2)</sup> has obtained credible results for 75 to 145 $\mu$ m thick electrodeposited (ED) copper foil between 23 and 175°. Similar results for 30.5 $\mu$ m ED copper foil have been obtained by Fu and Ume<sup>(3)</sup>. However, a more accurate characterization of elastic modulus (E) and yield stress ( $\sigma_y$ ), as well as of stress-strain ( $\sigma$ - $\epsilon$ ) curve in the elastoplastic region, requires a loading/unloading technique.<sup>(4)</sup>

No thermal expansion data for copper foil has been published, except average value of coefficient of thermal expansion ( $\alpha$ ) determined by Fu and Ume<sup>(3)</sup>. However,  $\alpha$  for bulk copper is temperature dependent above (and below) room temperature<sup>(7-11)</sup>, increasing from 16.5 x 10<sup>-6</sup>/deg C at 23° to 19 x 10<sup>-6</sup>/deg C at 300°C.

## Current Investigation

In this study, we have characterized annealed (180°C, 30 min.) 35 $\mu$ m copper foil, employing a micro-tensile tester<sup>(5)</sup> at 10<sup>-4</sup>/sec strain rate, in conjunction with non-contacting laser-speckle correlation technique described elsewhere<sup>(6)</sup>. Several loading/unloading stages, illustrated in Figure 1, produced E readings, with less than 5% scatter, which were averaged to develop a data point.

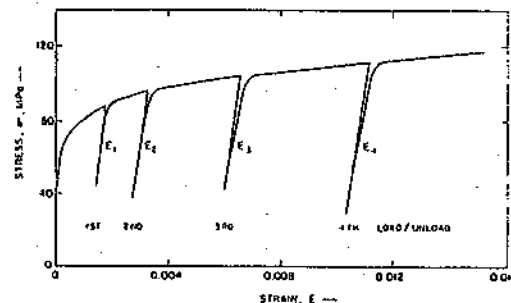


Figure 1: Loading / Unloading Procedure for Elastic Modulus Determination

In addition, we have determined  $\sigma_y$  (at 0.2% strain) and flow stress  $\sigma(1)$  (at 1% strain), both with less than 1% scatter; strain hardening parameter  $n$  and tangent modulus  $E_t = d\sigma/d\epsilon$  (slope of  $\sigma$ - $\epsilon$  curve) for  $\epsilon$  between 0.05 and 0.2%, the former by regression analysis. Monitoring the crosshead movement between 0.002 and 5 in/min, the strain-rate hardening parameter  $m$  was determined by regression. Figure 2 shows schematically the  $\sigma$ - $\epsilon$  diagram, effect of strain rate (crosshead speed) and the parameters E (elastic regime),  $E_t$ ,  $n$ ,  $m$ , (elastoplastic regime) and  $\sigma_y$ ,  $\sigma(1)$  (plastic regime).

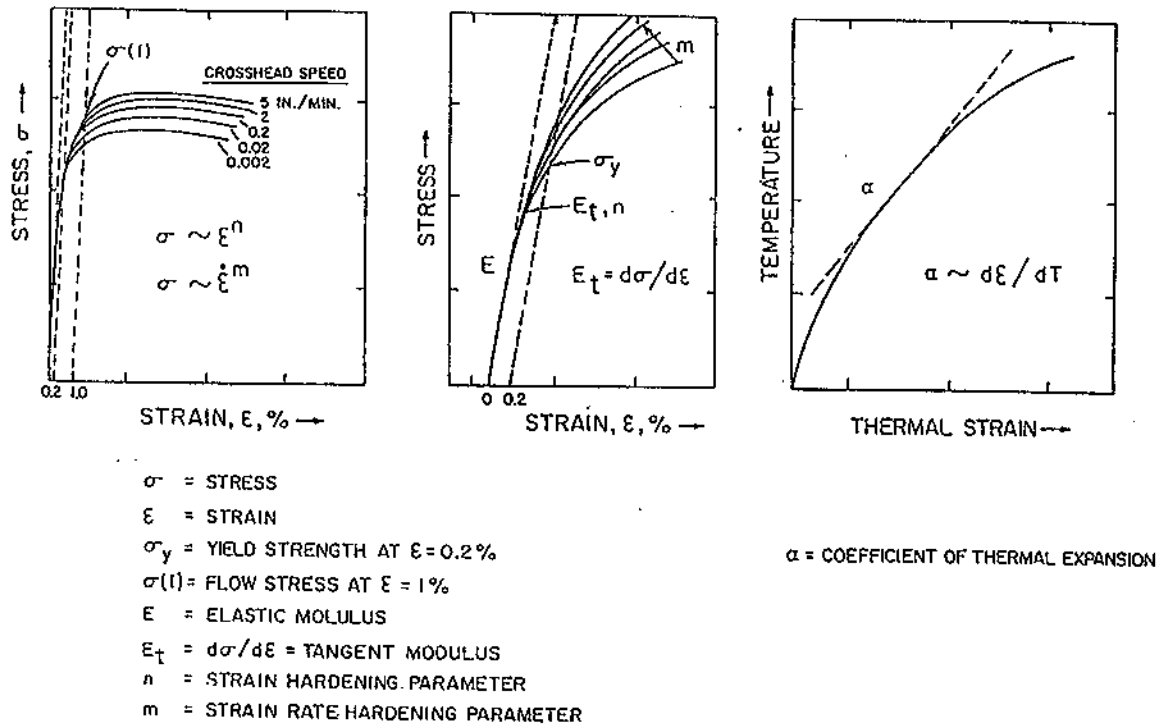


Figure 2: Schematic of Tensile Stress-Strain Curve and Elastic, Elasto - Plastic and Plastic Parameters

The thermal expansion was characterized using the same non-contact strain measurement technique<sup>(6)</sup>, monitoring cumulative thermal strain versus temperature over 23 – 300 °C range. The strain reading was read after equilibration for a few minutes. The NIST thermal expansion copper standard reference material SRM 736<sup>(12)</sup> was characterized in this fashion. For several repeat measurements, the scatter was less than 1.5%. Up to 225°C, the results conformed with the NIST standard expansion plot for copper. Above 225°C, some deviation from the standard curve ensued due to sample oxidation. This problem is being corrected.

For 35μm copper foils, thermal expansion curves up to 225°C were developed. For each foil, repeat measurements again yielded less than 1.5% scatter. Average expansion curve, averaged over data points from several measurements, was developed by fitting a polynomial to the expansion data<sup>(11)</sup>. Differentiation of the polynomial at a given temperature yielded temperature specific  $\alpha$ , as shown schematically in Figure 2.

## Results

Figure 3 shows the effect of test temperature on elastic modulus (E) and strain-hardening parameter (n). The foil grades are identified, the indicated average grain size was determined by planar TEM analysis of grain structure. The higher E and n at room temperature are apparently related to the smaller average grain size. However, the smaller grain size is also associated with a larger drop in E and n with temperature. Note that for the rolled and annealed GR8 foil, n and E are almost flat with temperature: n up to 300°C and up to about 200°C.

Figure 4 shows similar trends for yield stress  $\sigma_y$  and flow stress  $\sigma(1)$ . Note that at 23°C  $\sigma_y$  and  $\sigma(1)$  for the rolled foil GR8 are substantially lower than for the finer grained ED foils. At higher temperatures, this difference between the two foil types decreases.

Figures 5 and 6 show the effect of strain in the elasto-plastic region on tangent modulus ( $E_t$ ). As expected,  $E_t$  decreases rapidly with strain. The fine-grained ED foils have substantially higher  $E_t$  (than for the coarse-grained GR8 rolled foil). Note a very rapid diminution of  $E_t$  with

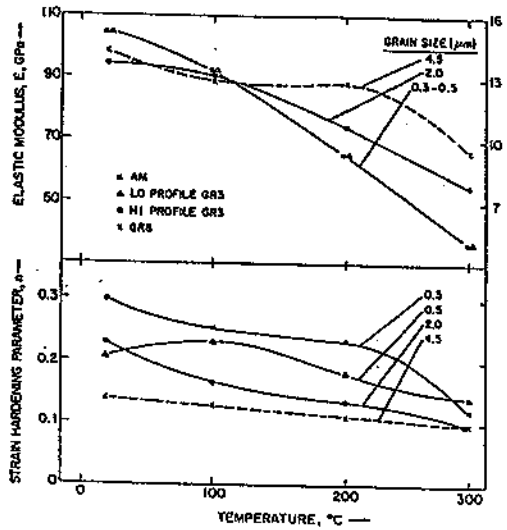


Figure 3: Effect of Temperature on Elastic Modulus and Strain Hardening Parameters for 35µm Copper Foils

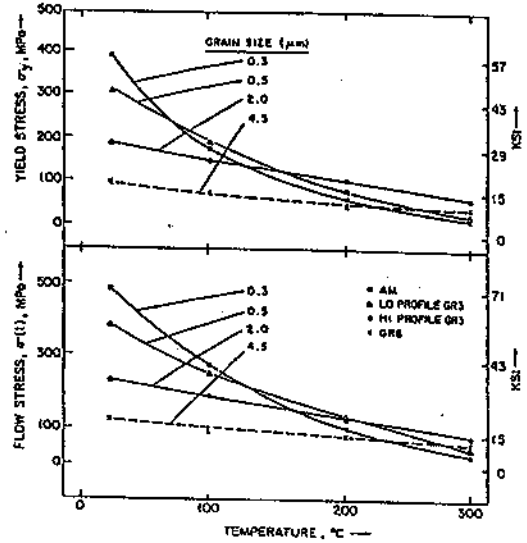


Figure 4: Effect of Temperature on Yield Stress and Flow Stress (at 1% Strain) for 35µm Copper Foils

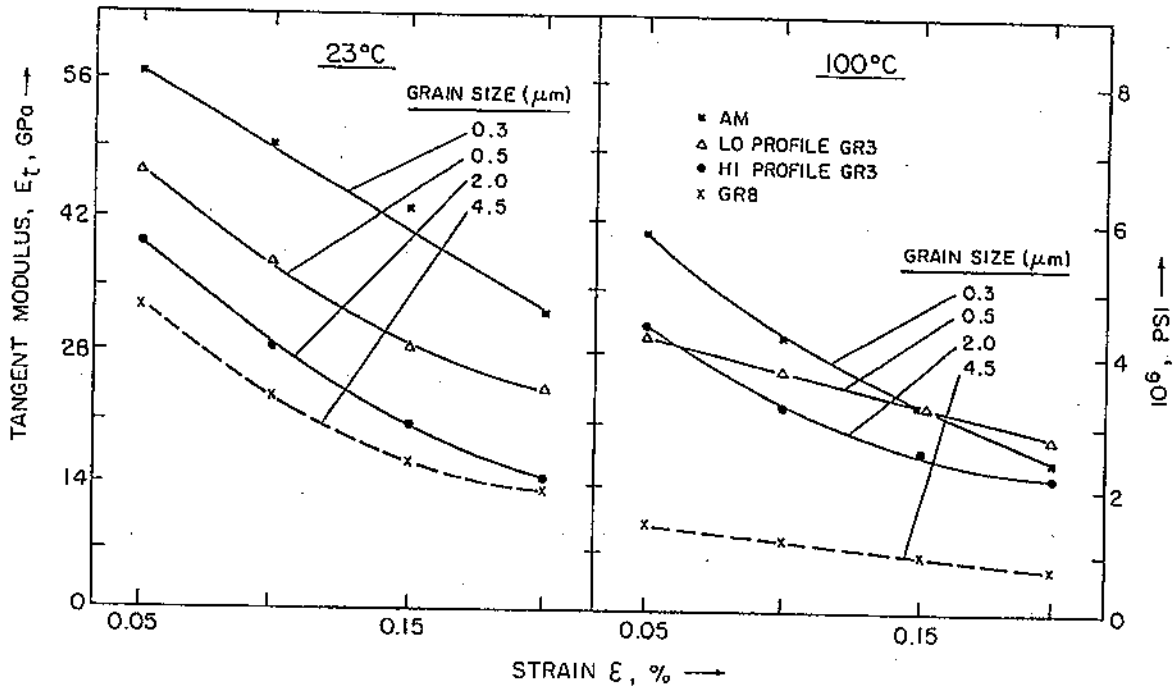


Figure 5: Effect of Strain in Elasto - Plastic Region on Tangent Modulus at 23°C and 100°C

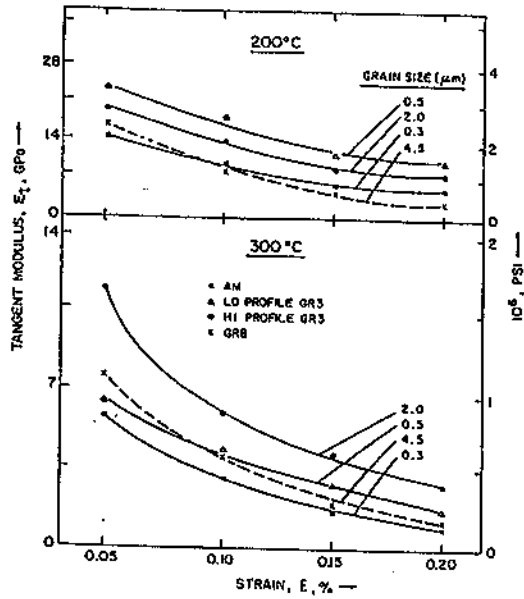


Figure 6: Effect of Strain in Elasto-Plastic Region on Tangent Modulus at 200°C and 300°C

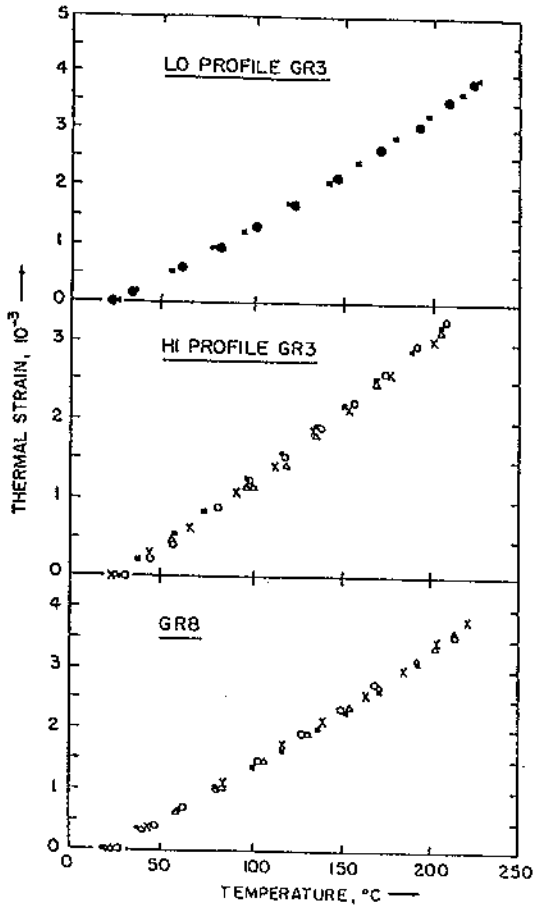


Figure 7: Effect of Temperature on Thermal Strain

temperature; at 300°C, intermediate grain size ED foil has the highest  $E_t$ .

Figure 7 shows the effect of test temperature on thermal strain  $E_t$  for the GR8 (rolled) and two GR3 (ED) type foils; the data points from several measurements are identified. Average lines through the data scatter for each foil are shown in Figure 8 where the fine-grained low profile GR3 has largest cumulative thermal strain between 23 and 225°C. A fourth-order polynomial was fitted to the data scatter and  $\alpha = (dE_t/dT)$  yielded temperature dependence of  $\alpha$ :

$$\alpha \times 10^6 = a_0 + a_1 T_1 + a_2 T^2 + a_3 T^3 + a_4 T^4 \dots (1)$$

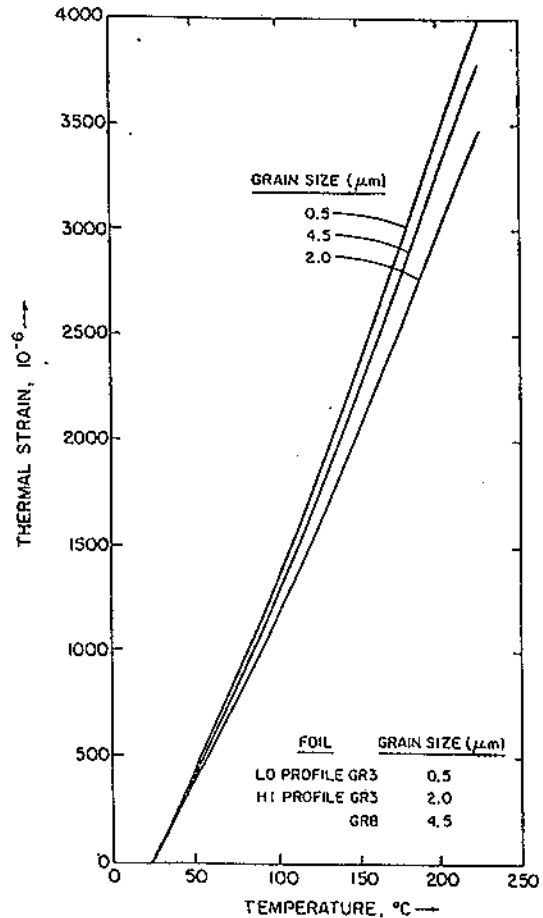


Figure 8: Comparison of Effect of Temperature on Thermal Strain for Three 35 $\mu\text{m}$  Copper Foils

Table 1  
Polynomial Parameters for  $\alpha$  (Equation 1)

Foil	$a_0$	$a_1$	$a_2$	$a_3$	$a_4$
GR8	$-4.1371 \times 10^2$	$1.7957 \times 10^1$	$3.8218 \times 10^{-3}$	$-5.7953 \times 10^{-5}$	$2.8699 \times 10^{-7}$
Lo Prof. GR3	$-3.8090 \times 10^2$	$1.6435 \times 10^1$	$1.1814 \times 10^{-2}$	$-6.5461 \times 10^{-5}$	$2.9235 \times 10^{-7}$
Hi Prof. GR3	$-367.98 \times 10^6$	$131170 \times 10^2$	$579 \times 10^2$	$-3.4562 \times 10^2$	$8.0135 \times 10^{-1}$

Table 1 shows the parameters  $a_0, a_1, a_2, a_3, a_4$  for the three foils and Figure 9 illustrates the effect of temperature on  $\alpha$ . The intermediate grain size, high profile GR3 foil has the lowest  $\alpha$  over the 23 - 225°C temperature range. However, the remarkable aspect of temperature trend is rapid rise of  $\alpha$  above a critical temperature somewhere between 100 - 150°C.

Figure 10 compares the temperature dependency of E and  $\alpha$  for the GR8 rolled foil with that for the 6mm bulk material. The grain size for bulk material is not available but it should be at least an order of magnitude greater. Both E and  $\alpha$  trends deviate for the foil and bulk materials, the deviation is especially pronounced for  $\alpha$ , and is attributable in part to the grain boundary contribution to E<sup>(13,4)</sup> and  $\alpha$ <sup>(15)</sup>. This contribution increases with decreasing grain size.

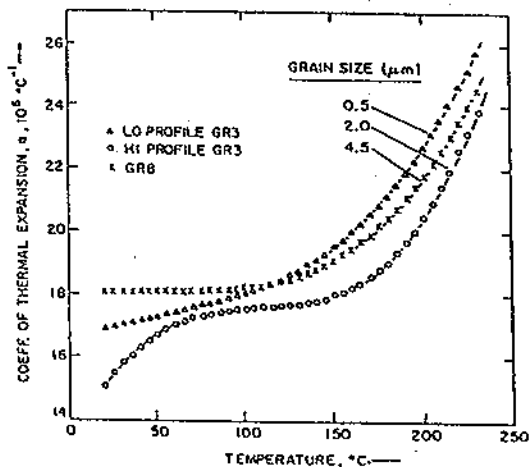


Figure 9: Effect of Temperature on Coeff. of Thermal Expansion for Three 35µm Copper Foils

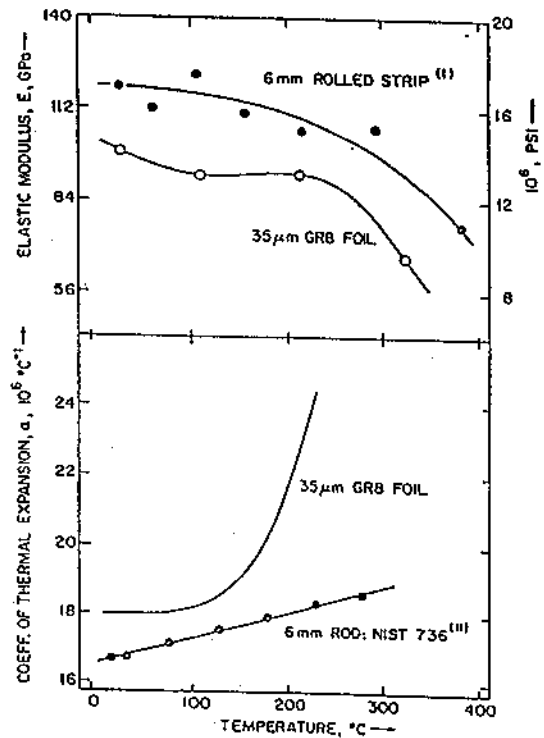


Figure 10: Comparison of Temperature Dependency of Elastic Modulus and Coefficient of Thermal Expansion for Rolled 6mm Bulk Material and 35µm Rolled Foil [Bulk Material Data from References (1) and (11)]

### Discussion

Considerable amount of finite element analysis (FEA) work is currently underway at various industrial and academic R/D centers to address the issues of warp, curl, wrinkle and internal stresses in foil, laminate and circuit boards. Often the room temperature handbook values of elastic modulus and thermal expansion are utilized. The thrust of this study is to provide a more realistic elastic and thermal parameters for the FEA models. As we have observed in the previous section, E and  $\alpha$  are unique to a foil type and they vary with temperature more critically for thin foil than for bulk material.

Additional elastoplastic ( $n, m, E_s$ ) and plastic [ $\sigma_y, \sigma(1)$ ] parameters can be derived from the stress-strain response; these parameters play important roles in the foil and laminate performance. An overview of connection between these parameters and performance is summarized in Table 2. The preliminary results for experimentally (crosshead movement) determined strain rate hardening parameter  $m$  for three ED foils is presented in Table 3. Note that the  $m$  values for ED foils are considerably higher than those encountered for thick rolled sheet<sup>(16-18)</sup>, perhaps attributable to high concentration of point defects in ED foils. Utilizing first order analytical relationships and tensile and thermal parameters, an approximate quantification of several performance issues is presented below.

Table 2  
Foil/Laminate Performance Related to Tensile Parameters

Foil/Laminate Performance	Parameter(s)
Cracking	$\sigma_u, \epsilon_t$
Denting	$\sigma_y$
Wrinkling	$E_s$
Warpage/Curl	$E, \alpha$
Drawability	$n$
Necking, Formability	$m, n$

\* $\sigma_u$  = Ultimate Strength,  $\epsilon_t$  = Total Elongation

Table 3  
Strain Rate Hardening Parameter ( $m$ ) for Three Annealed (180°C, 30 min) ED Foils for Strain  $\epsilon = 0.1 - 0.3\%$

Foil: →	AM	Lo Prof. GR3	Hi Prof. GR3
Grain Size ( $\mu\text{m}$ ): →	0.3	0.5	2.0
23°C	0.075	0.041	0.028
100°C	0.099	0.065	0.043
180°C	0.135	0.098	0.063
200°C	0.144	0.104	0.080

### (i) Thermal Stress<sup>(19)</sup>

When a metal straddling a substrate is cooled through temperature differential  $\Delta T$ , a thermal stress  $\sigma_c(T)$  is generated. For  $t_s E_s / (1 - \nu_s) \gg t_c E_c / (1 - \nu_c)$ , where  $t$  is thickness,  $\nu$  is Poisson's ratio and subscripts  $s$  and  $c$  are for substrate and coating (or metal) respectively.

$$\sigma_c(T) = (\alpha_s - \alpha_c) \Delta T E_c (1 - \nu_c)^{-1} \dots (2)$$

Note  $\sigma_c$  is independent of  $t_c, t_s$  or  $E_s$ ; a higher  $E_c$  generates a larger  $\sigma_c(T)$ . For  $t_c E_c / (1 - \nu_c) \gg t_s E_s / (1 - \nu_s)$ ,

$$\sigma_c(T) = (\alpha_s - \alpha_c) \Delta T (t_s / t_c) E_s (1 - \nu_s)^{-1} \dots (3)$$

Note that  $\sigma_c$  is independent of  $E_c$  but is dependent on  $E_s$  and thickness ratio  $t_s / t_c$ ; thinner coating generates larger  $\sigma_c$ . When  $t_c$  and  $t_s$  are comparable,  $\sigma_c$  is again independent of  $t_s, t_c$  but depends only on  $E_s$ . In either case,  $\sigma_c$  is controlled by the elastic properties ( $E_s, \nu_s$ ) of the substrate. For  $18\mu\text{m}$  Cu on  $100\mu\text{m}$  FR-4 cooled from  $180^\circ\text{C}$ ;  $0.2\mu\text{m}$  Cu on  $25\mu\text{m}$  polyimide (PI) or  $0.02\mu\text{m}$  Cr on  $25\mu\text{m}$  PI cooled from  $200^\circ\text{C}$ , calculations show that about 8 ksi (55 MPa)  $\sigma_c$ , driven entirely by  $\Delta T$  and  $\Delta\alpha$ , is generated. If  $\alpha_s > \alpha_c$ , the metal is residually compressed and the substrate is in residual tension.

### (ii) Curl<sup>(19)</sup>

Thermal stress  $\sigma_c$  at the metal (coating)/substrate interface results in a bending moment and subsequent bowing of the c-s composite. When  $t_s \gg t_c$  and for  $t_s E_s / (1 - \nu_s) \gg t_c E_c (1 - \nu_c)$ , for c-s cantilevered at length  $l$ , the curl  $\delta$  is given as:

$$\delta = 3l^2 (\alpha_s - \alpha_c) \Delta T \frac{E_c}{E_s} \left[ \frac{1 - \nu_s}{1 - \nu_c} \right] \frac{t_c}{t_s^2} \dots (4)$$

Thick coating and thin substrate enhance  $\delta$ , the effect of substrate dimension is particularly pronounced. Likewise, substrate with low modulus and high thermal expansion facilitates curl; metal with low modulus and high thermal expansion suppresses curl.

For comparable  $t_s$  and  $t_c$ ,

$$\delta = 3l^2 (\alpha_s - \alpha_c) \Delta T t_s (t_s + t_c) E_s \left[ \left( \frac{1 - \nu_s}{1 - \nu_c} \right) E_s t_s^2 + (E_s t_s^2) \right] \dots (5)$$

Both metal and substrate in concert reduce curl, the contribution of substrate in resisting  $\delta$  is greater. Reducing copper thickness by etching following lamination tends to increase  $\delta$ , the contribution of Cu in resisting  $\delta$  is reduced further. A high  $E$ , low  $\alpha$  substrate is prone to show significantly lower  $\delta$ . We note that  $\sigma_c$  is usually less than yield stress and neither ultimate strength or elongation of copper play any part in the resulting  $\delta$ .

(iii) Warpage <sup>(19-20)</sup>

Arguments of (i) and (ii) also apply to warpage in two-layer or multi-layer laminate or circuit board. Internal compressive stresses in the metal layer bend the substrate concavely upward. Sometimes when the stresses are too large, the metal layer may wrinkle or delaminate (largely elastic response) if in compression or may fracture if in tension (here tensile properties at room and high temperatures are relevant). The magnitude of bending moment  $M$  for a sample of width  $w$  is

$$M = \frac{1}{2} \sigma_c t_c w (t_c + t_s) \quad \dots (6)$$

$M$  is directly related to  $\sigma_c$  and  $w$ . It also depends upon laminate thickness  $t_c + t_s$ ; the effect of metal thickness, however, is greater. When the metal layer straddles a higher  $\alpha$  substrate, during cooling  $M$  thrusts the laminate convexly towards the lower  $\alpha$  metal layer.

A balanced laminate construction, (a) equal layer thickness of same metal on both sides of substrate or (b) equal  $\sigma_c t_c$  (or  $E_c t_c$ ) of different metals on each side, results in two equal and opposite bending moments and zero net warp. Anneal softening of one of the two layers of two-sided laminate sometimes causes warp. This may happen only if (c) anneal induced recrystallization and/or softening in one layer reduces or eliminates intrinsic internal stresses or (d) annealing reduces elastic modulus to a significant extent. Either (c) or (d) may result in a net non-zero bending moment and hence the warp.

It is possible to suppress the net bending moment causing warpage by cooling under pressure; or to balance the bending moment by symmetrical construction. However, for either case, the thermal stresses at the Cu/FR-4 interface remain intact. For the former, subsequent heating during processing or in service can restore the bending moment and cause warpage. For the latter, partial or complete etching (or uneven thickness on either side after etching) can generate unbalanced bending moments and hence the warpage.

The PWB warpage can be modeled by the knowledge of (a) temperature dependence of the material properties and (b) solid/applied mechanics using the three-dimensional thermoelastic or thermo-viscoelastic analysis. In

practice, however, this is difficult. Viscoelastic or plastic relaxation (reduction of residual stresses) may occur at the peak lamination or soldering temperatures. Warpage may occur due to thermal loading during the reflow or infrared soldering and during the solder-masking process. The temperature gradients through the board thickness contribute most substantially to the total warpage. Support conditions of the board, that is, the behavior of the curvature of the board parallel to the support axis is another uncertainty.

The laminate layers are deposited at different temperatures and therefore not all layers are stress-free at the same temperature. Further, the residual stresses might develop due to plastic deformation, under a large thermal load, at an intermediate process step. Hence, the warpage should be considered at the intermediate process steps as well as at the end of fabrication. Clearly, these complexities cannot be captured by the "frozen-view" models; it is important to take into account the entire history of the fabrication process and the evolution of internal stresses to understand the thermo-mechanical behavior of multi-layer PWB. Optimum material properties, PWB geometry and lamination/masking/soldering process parameters must be selected to minimize warpage.

(iv) Three-Layer Model <sup>(19, 20)</sup>

An analysis of stress and strain distributions for a three-layer Cu/FR-4/Cu, layers 1, 2, 3 respectively, construction, when the laminate is cooled through a temperature differential  $\Delta T$ , has yielded predictive relationships for warpage, dimensional stability and thermally induced stresses (in core and copper):

Warpage:

$$\frac{\delta}{l} = \frac{3}{2} \frac{t_2 E_2 (\Delta T) (E_3 - E_1) (\alpha_1 - \alpha_2) (t_1^2 + t_2^2)}{(E_3 + E_1) (t_1 E_1 + t_2 E_2 + t_1 E_3) [2(t_1 + t_2) - t_2^2]} \quad \dots (7)$$

Dimensional Stability:

$$\frac{\Delta X}{x_0} = (\Delta T) (\alpha_1 - \alpha_2) \left[ 1 + \frac{E_2 t_2}{2 E_1 t_1} \right]^{-1} \quad \dots (8)$$

Maximum Stress in Copper (at edges of plate or stripe):

$$\sigma_{\max} = (\Delta T)(\alpha_1 - \alpha_2)E_1 \left[ 1 + \frac{(t_1 + t_2)E_1}{t_1 E_2} \right]^{-1} \quad \dots(9)$$

Maximum Shear Stress in Core (in the center area of the board):

$$\tau_{\max} = (\Delta T)(\alpha_1 - \alpha_2) \left[ \frac{t_1 E_1 E_2}{t_2 (1 + \nu)} \right]^{1/2} \left[ 1 + \frac{2t_1 E_1}{t_2 E_2} \right]^{-1} \quad \dots(10)$$

Substituting appropriate values of  $(\Delta T)$ ,  $l$ ,  $t$ ,  $\alpha$ ,  $E$  and  $\nu$ , reasonable predictive evaluations of warpage, dimensional change and thermal stresses are obtained for symmetrical, unsymmetrical and one-sided laminates. Effects of variations in core thickness ( $t_2$ ),  $E$ ,  $\alpha$ , lamination cycle and foil thickness ( $t_1$ ,  $t_3$ ) can be predicted. For more sophisticated treatment of thermomechanical analysis see reference (21). Special attention is drawn to modeling and finite element analysis work underway at Georgia Institute of Technology.<sup>(22-27)</sup>

#### (v) Wrinkling and Denting<sup>(28-31)</sup>

Under conditions of non-uniform loading, wrinkles and dents start with strain instability and stress concentration at selected points on the foil. At points of instability, elastic or elastoplastic buckling is brought on by in-plane compressive stress component of a complex stress state. Initiation of wrinkles corresponds to elastic response (and instability), onset of visible wrinkles to elasto/plastic response and growth of wrinkles (and dents) to plastic response. As the foil thickness decreases, the onset of wrinkles is observed at less than 1% strain and the wrinkle shape becomes irregular. The onset and growth of macroscopic wrinkling occurs when the stress exceeds a critical value

$$\sigma_{cr} = 0.33(1 - \nu)^{-1} (t/w)^2 j E_0 \dot{\epsilon} \quad \dots(11)$$

where  $j$  is function of foil dimensions and  $E_0$  is wrinkling modulus defined as

$$E_0 = 4EE_1 \left[ E^{1/2} + E_1^{1/2} \right]^{-2} \quad \dots(12)$$

The parameters  $E$ ,  $E_1$  and  $\nu$  in equations (11) and (12) are derived from the stress-strain test

conducted at strain rate  $\dot{\epsilon}$ . For high  $\sigma_{cr}$  material, strain for onset of wrinkles is low and vice versa. Increase in elastic modulus and yield strength results in numerous shallow wrinkles formed at small strain. As temperature is increased, both yield strength and elastic modulus decrease; the result is that fewer wrinkles are formed and they form at larger strain. High  $n$  and  $m$  ( $m$  is of secondary importance) and low  $\dot{\epsilon}$  increase the strain for onset of wrinkling and the initiation of wrinkling is diminished. For high  $n + m$ , ( $m$  is of primary importance), high  $\sigma_y$  and low  $\dot{\epsilon}$ , growth of wrinkles (once formed) is retarded.

As a general rule, the material with high  $n$  and  $m$  will have low tendency to wrinkle and dent. High  $E_0$  and  $\sigma_{cr}$  are also indicators of low propensity to wrinkle or to dent. The factors which impart flexibility (as opposed to stiffness) to the foil, such as decreasing  $E$  and  $\alpha(1)$ , will also render foil less prone to wrinkling. Low  $\dot{\epsilon}$  employed during service will decrease handling damage.

#### Acknowledgements

Thermo-mechanical formulation of three-layer laminate was conducted by Prof. E. El-Magd. Thermal expansion characterization was done by P. Zimprich. The strain-rate hardening parameter ( $m$ ) for ED foils by crosshead monitor were characterized by Mel Minor, Gould Electronics.

#### References

- (1) W. H. Munse and N. A. Weil, "Mechanical Properties of Copper at Various Temperatures", ASTM Proc. 51 (1951) 996 - 1018.
- (2) A. Fox, "Mechanical Properties at Elevated Temperature of Cu Bath Electrodeposited Copper for Multilayer Boards", J. Testing and Evaluation 4, (1976) 74 - 84.
- (3) C. Y. Fu and C. Ume, "Characterizing the Temperature Dependence of Electronic Packaging - Material Properties", JOM 47 (1995) 31 - 35.
- (4) C. A. O. Henning, F. W. Boswell and J. M. Corbett, "Mechanical Properties of Vacuum-Deposited Metal Films - I. Copper Films", Acta Metallurgica 23 (1975) 177 - 185.
- (5) Metphysik Furstenfeld, Austria.
- (6) M. Anwander, B. Weiss, B. Zagar and H. Weiss in "Experimental Mechanics" (Ed. I. M. Allison), 1998, Balkema, Rotterdam, 692 - 702.
- (7) T. A. Hahn, "Standards, Copper, Methods: Thermal Expansion of Copper From 20 to

- 800 K – Standard Reference Material 736”, *J. Appl. Phys.* 41 (1970) 5096 – 5101.
- (8) A. J. Pojour and B. Yates, “Thermal Expansion at Elevated Temperatures 1: Apparatus for Use in the Temperature Range 300 – 800K: The Thermal Expansion of Copper”, *J. Scientific Instruments* 6 (1973) 63 – 66.
  - (9) T. G. Kollie, D. L. McElroy, J. T. Hutton and W. M. Ewing “A Computer Operated Fused Quartz Differential Dilatometer”, in *Thermal Expansion – 1973*, AIP Conf. Proc. 17, American Institute of Physics, 1974, 129 – 146.
  - (10) S. J. Bennett, “The Thermal Expansion of Copper Between 300 and 700 K”, *J. Phys. D: Appl. Phys. II* (1978) 777 – 780.
  - (11) G. K. White and R. B. Roberts, “Problems in Presenting Key Values: Linear Expansivity of Copper”, *High Temperatures – High Pressures* 12 (1980) 311 – 316.
  - (12) The copper thermal expansion standard material SRM 736 may be ordered from the Office of Standard Reference Materials, National Institute of Standards and Testing (NIST), Washington, DC 20234.
  - (13) V. Krstic, U. Erb and G. Palumbo, “Effect of Porosity on Young’s Modulus of Nanocrystalline Materials”, *Scripta Metallurgica et Materialia* 29 (1993) 1501 – 1504.
  - (14) X. J. Wu et al, “Synthesis and Tensile Property of Nanocrystalline Metal Copper”, *Nanostructured Materials* 12 (1999) 221 – 224.
  - (15) H. J. Klam, H. Hahn and H. Gleiter, “The Thermal Expansion of Grain Boundaries”, *Acta Metallurgica* 35 (1987) 2101 – 2104.
  - (16) A. K. Ghosh, “Influence of Strain Hardening and Strain Rate Sensitivity on Sheet Metal Forming”, *Trans. ASME* 99 (1977) 264 – 274.
  - (17) A. M. Szacinski and P. F. Thomson, “Effect of Mechanical Properties on the Wrinkling Behavior of Sheet Materials in the Yoshida Test”, *J. Mech. Working Technology* 10 (1984) 87 – 102.
  - (18) R. Mahmudi, “Forming Limits in Biaxial Stretching of Aluminum Sheets and Foils”, *J. Materials Processing Technology* 37 (1993) 203 – 216.
  - (19) H. D. Merchant, “Warp and Curl in Cu/FR-4 and Cu/PI Laminates”, Internal Report, Gould Electronics, Feb. 18, 2000, 7 p.
  - (20) R. Wiechmann, “Thermally Induced Warp of Thin Laminates”, Gould Electronics Internal Report, Oct. 1, 1999, 12 pp.
  - (21) J. H. Lau, “Thermal Stress and Strain in Microelectronics Packaging”, Van Nostrand Reinhold, 1993, 383 pp.
  - (22) I. C. Ume, T. Martin and J. T. Gatro, “Finite Element Analysis of PWB Warpage Due to Solder Masking Process”, *IEEE Trans, CPMT, Part A* 20 (1997) 295 – 306.
  - (23) I. C. Ume and T. Martin, “Finite Element Analysis of PWB Warpage Due to Cured Solder Mask – Sensitivity Analysis”, *IEEE Trans., CPMT, Part A* 20 (1997) 307- 316.
  - (24) Y. Polsky, I. C. Ume and W. Sutherland, “Application of Thermoelastic Lamination Theory of a Symmetric and Simply Supported Pointed Wiring Board During Temperature Cycling”, *Proc., Electronic Components and Technology Conference, IEEE, Seattle, May 1998*, 345 – 352.
  - (25) G. J. Petriccione and I. C. Ume, “Warpage Studies of HDI Test Vehicles During Various Thermal Profiling”, *IEEE Trans., Advanced Packaging* 22 (1999) 125 – 632.
  - (26) Y. Polsky and I. C. Ume, “Thermoelastic Modeling of a PWB with Simulated Circuit Traces Subjected to Infrared Soldering”, *J. Electronic Packaging* 121 (1999) 263 – 270.
  - (27) M. N. Variyam, W. Xie and S. K. Sitaraman, “Role of Out-of-Plane Coefficient of Thermal Expansion in Electronic Packaging Modeling”, *J. Electronic Packaging* 122 (2000) 121 - 127.
  - (28) I. Aoki, T. Matoba and M. Ataka, “Effect of Mechanical Properties on the Growth of Wrinkles in Sheet Metal Forming”, *Proc. 12<sup>th</sup> Biennial Congress, Inter. Deep Drawing Research Group, Santa Margherita Ligure, Italy, May 1982*, 221 – 229.
  - (29) A. M. Szacinski and P. F. Thomson, “Effect of Mechanical Properties on the Wrinkling Behavior of Sheet Materials in the Yoshida Test”, *J. Mechanical Working Technology* 10 (1984) 87 – 102.
  - (30) A. M. Szacinski and P. F. Thomson, “Initiation of Buckling in Anisotropic Metal Sheet” *Adv. Tech. Plasticity* 11 (1987) 1171 – 1178.
  - (31) A. M. Szacinski and P. F. Thomson, “Wrinkling Behavior of Aluminum Sheet During Forming at Elevated Temperature” *Mats. Sc. Tech.* 7 (1991) 37 – 41.